DOI No.: 10.5963/IJMT0102004
International Journal of Multimedia Technology IJMT

A No-Reference Objective Image Sharpness Metric Based on a Filter Bank of Gaussian Derivative Wavelets

Chengho Hsin*, Jr-Wei Jang, Shaw-Jyh Shin, Shin-Hsien Chen;
Department of Communications Engineering;
Feng Chia University, Taichung, Taiwan;
chhsin@fcu.edu.tw*

Abstract-**The purpose of this paper focuses on the development of a no-reference objective image sharpness (or blurriness) metric. A high-frequency component preserving the full information of a given input image is extracted first and then is applied to a multi-channel filter bank designed by a snug wavelet frame composed of the Gaussian derivatives. The output of the filter bank not only contains the complete information of the input but also manifests prominent image features. The proposed method measures image sharpness based on the output of this filter bank. Experimental results show that the metric predicts well in isotropic and uniform blur case. Validated by the high correlation between the metric values and the subjective test scores, the performance of the proposed metric is comparable to that of human subjects.**

Keywords- sharpness metric; blurriness metric

I. INTRODUCTION

Image quality assessment is indispensable to various image processing applications such as compression, transmission, enhancement, restoration, printing, display, and analysis. Although subjective quality assessment is considered to be the most accurate and reliable approach it is expensive and time-consuming and is inappropriate for real-time implementation.

The development of objective metrics that can precisely predict the perceived image quality is in great demand. Objective metrics can be categorized into full-reference, reduced reference, and no-reference [1]. A reference such as the original image is needed for comparison with the processed image in the full-reference scheme. Reduced-reference objective metrics only require partial information about the original image. In many circumstances, the reference image is not available for the assessment task. Hence, objective metrics using the reference image impose a limitation on their applications. On the other hand, a no-reference metric scheme computes the perceived visual quality directly from a given image without referring to the reference image. It is much more useful than the other two categories. Image quality is governed by a variety of factors such as sharpness, naturalness, colorfulness, contrast, and noise etc. To develop a no-reference objective image quality metric by incorporating all attributes of images without referring to the original ones is a difficult task. Hence, we shall concentrate on the work of the no-reference image sharpness (or blurriness) metric. Note that the image sharpness metric can also be applied to measure blurriness since they are inversely related.

A general review of no-reference objective image sharpness/blurriness metrics were given in [2]. Only recent methods with high performance results are described here. They can be divided into transform-based [3-9], edge-based [2, 10-15], space and spectrum based [16, 17], and learning-based [18, 19] approaches. Marichal et al. [3] developed a global blur metric based on the occurrence histogram of non-zero DCT coefficients among all the 8×8 blocks of a frame. The method is therefore directly applicable in compressed domain. The correlation between the blur metric and the subjective test scores were not conducted. Wee and Paramesran [4] formulated the problem of image sharpness metric as a generalized eigenvalues problem. A covariance matrix is computed from an energy-normalized input image. The image sharpness is then determined by the trace of the first several eigenvalues of this matrix. Similarly, a sharpness metric proposed by Maalouf and Larabi [5] makes use of a wavelet-based multiscale Di Zenzo structure tensor. The difference of the eigenvalues of the multiscale structure tensor is used to measure the sharpness of color edges. Zhu and Milanfar [6] computed sharpness metric in the presence of both noise and blur using the singular values of the local image gradient matrix. They assumed that the noise variance is known in advance. Wang and Simoncelli [7] first pointed out that the blurring of an image results in the disruption of its local phase. They demonstrated that precisely localized features such as step edges have strong local phase coherence structures across scale and space in the complex wavelet transform domain, and blurring causes loss of such phase coherence. Both [8] and [9] have developed image blur metrics based on local phase coherence measurement. The test results given by [9] have shown high correlation with subjective quality evaluations. In general, the transform-based methods described in the above are computation demanding.

Blurring causes the widening of the original edge profiles in an image. The key concept of edge-based blur metrics therefore is to analyze the distribution of various edge profiles. Tong et al. [10] applied Harr wavelet transform to find edges in a given image. By discriminating different types of edges, the method could determine whether an image is blurred or not and to what extent an image is blurred. Metrics [2, 11-15] rely on the determination of the edge width to evaluate the amount of blur. These methods first find edge pixels using common edge detectors. The start and end positions of the edge for each edge

pixel are found. The edge width is computed as the distance between the end and start positions. Marziliano et al. [11] have derived the overall blur metric as the average widths of the edges. Ong et al. [12] have applied the average of the edge spread to an exponential model to calculate the blur metric. The parameters of the exponential model must be estimated by a training process. Ferzli and Karam [2] pointed out that the previous two methods are unable to predict the relative amount of blurriness in images with different content. Hence, they proposed an image sharpness metric based on the notion of just noticeable blur (JNB). The JNB is the minimum amount of perceived blurriness around an edge given a contrast higher than the just noticeable difference. The probability of detecting a blur distortion is determined by the edge width soft thresholded with the corresponding JNB. The block-based probability summation model is adopted to compute the sharpness metric. It was shown in [13] that the results of the JNB method do not correlate well with subjective scores for images with non-uniform saliency content. To solve this problem, Sadaka et al. [13] proposed a saliency-weighted sharpness metric, where the saliency map is obtained by a computational visual attention model. On the other hand, Narvekar and Karam [14] developed a sharpness metric based on a cumulative probability of blur detection (CPBD) to improve the JNB method. Liang et al. [15] proposed a similar approach to measure the sharpness by extracting the gradient profiles of the edge points. A so-called the gradient profile sharpness histogram in conjunction with the just noticeable distortion (JND) threshold is used to evaluate the blurring artifacts and assess the image quality.

The space and spectrum based sharpness metrics gather features from both domains to assess the image quality. Caviedes and Oberti [16] developed a content independent sharpness metric based on the local frequency spectrum around the image edges. The average 2D kurtosis of the 8×8 DCT blocks is used to measure sharpness. Vu and Chandler [17] proposed a block-based algorithm, named S_3 metric, designed to measure the local perceived sharpness in an image. For each block, a spectral sharpness measure is determined by the slope of the magnitude spectrum and a spatial sharpness measure is calculated by the total spatial variation. A perceived sharpness map is generated by combining the two measures via a weighted geometric mean. The overall sharpness of an image is obtained by the maximum value of the sharpness map.

Learning-based methods attempt to increase the performance of the existing blur metrics by incorporating the appropriate prior information into the training process. Ciancio et al. [18] proposed a paradigm for blur assessment that combines different metrics and low-level image features in a classifier based on a neural network structure. A large real image database was built for testing the paradigm, together with the ground truth associated to these images which was obtained by subjective tests. Chen and Bovik [19] developed a three-step algorithm which operates in a coarse-to-fine manner. First, a probabilistic support vector machine (SVM) is applied to classify an image into either as "sharp" or as "blur" by evaluating the distance between the gradient statistics of the image and a statistical model of natural scenes. Then a wave let decomposition is used to refine the blur assessment. Finally, the blur information is pooled to predict the blur quality of images. Both learning methods have shown the above average performance in correlation with human subjectivity but room for improvement remains.

In summary, the edge width may not be accurately measured in a moderately blurred image with a simple edge detector [20]. Many edges might go undetected in a highly blurred image with a single scale edge detector. As a result, only a portion of edge pixels carry information about the sharpness of the image. Therefore, edge-based metrics become less correlated with the perceived sharpness as the amount of blur increases. Utilizing both spectral and spatial properties of the image to generate a block-based sharpness map is a representative of non-edge based approach [16, 17]. However, the way of merging the two types of the properties and the size of blocks for computing the properties might affect the performance of the algorithm.

In this paper, we propose a no-reference objective image sharpness metric based on a filter bank of Gaussian derivative wavelets. The proposed metric does not require edge detection, block-wise computation, and learning process. Multi-channel filter bank structure is applied to extract spectral and spatial properties as integral attributes. Furthermore, the Gaussian derivatives are designed to obtain edge information contained in an image. It is shown that the proposed metric can accurately predict the perceived sharpness of highly blurred images.

The paper is organized as follows. Section II presents the filter bank of Gaussian derivative wavelets which lays the foundation for the proposed metric. The procedure of measuring the sharpness metric is described in Section III. Performance results are presented in Section IV. A conclusion is given in Section V.

II. A FILTER BANK OF GAUSSIAN DERIVATIVE WAVELETS

A filter bank realizes the proposed metric was developed in [21]. The primary motivation of using Gaussian derivatives is that they are able to describe almost all attributes of a given image. Furthermore, the wavelet transform provides multi-resolution space-frequency analysis. A redundant isotropic filter bank derived from a three-voice snug Gaussian derivative wavelet frame is shown in Fig. 1. This filter bank is composed of a band-pass channel and a low-pass channel. The impulse response of the band-pass channel is given by

$$h(m,n)=\left\{\sum_{p=1}^{3}(-1)^{p}R_{p}\nabla^{2p}g(x,y;\eta_{p})\right\}x=m,y=n \tag{1}$$

where m and n are integer indexes, $\nabla^{2p}=\left(\frac{\partial^2}{\partial x^2}+\frac{\partial^2}{\partial y^2}\right)^{p}$ is the *pth*-order Laplacian operator, and $g(x,y;\eta_p)=\frac{1}{2\pi\eta_p}\exp(\frac{-(x^2+y^2)}{2\eta_p^2})$. The impulse response of the low-pass analysis filter is expressed by $h_0(m,n)=R_0 g(m,n;\eta_0/\sqrt{2})$. The parameters η_p and R_p are specified in TABLE I. Both band-pass filter

$h(m,n)$ and low-pass filter $h_0(m,n)$ are isotropic. A down-sampler appears only at the end of the low-pass analysis filter. The filter bank can be easily expanded to multiple levels for the purpose of multi-resolution decomposition. In fact, because the filter bank is redundant, the original image $f(m,n)$ can be perfectly reconstructed from the output of the band-pass channel $q(m,n)$ plus the average (or DC) value of the image by a conjugate gradient algorithm. Hence, it is clearly indicated that the band-pass filter image $q(m,n)$ contains complete information of the original image except the average level of the image.

TABLE I. THE PARAMETERS OF GAUSSIAN DERIVATIVE FILTERS

order	p=0	p=1	p=2	p=3
R_p	2	1.451892	1.45103	0.2383
η_p	1.7563	1.8014	1.6371	1.1758

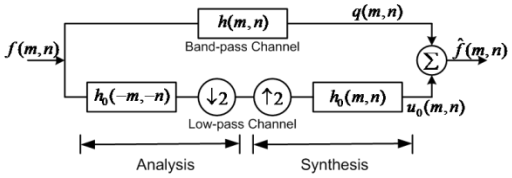

Figure 1. A filter bank of Gaussian derivative wavelets.

III. PROPOSED NO-REFERENCE SHARPNESS METRIC

The procedure of computing the proposed sharpness metric is as follows. Firstly, the input image is adjusted to a square size. Blur in an image is due to the attenuation of high spatial frequency component. Thus, it is logical to extract the high frequency component of the processed image and then send it to the multi-channel filter bank for the sharpness metric computation.

A. Adjusting Image to Square Size

The central part of an image is usually the starting point for human visual attention. Let $M = 2^L$, and L be the minimum integer that satisfies $M \geq \max(length, width)$. The initial input image is cut into a square size with length M measured from the center point of the image. The empty region of the square image is mirrored from the original image. A square image is necessary for subsequent multi-channel decomposition.

B. Computing Global Band-Pass Image Contrast

Fig. 2 shows that the high-frequency component is obtained by the difference between the input square image and its low-pass image. That is $d(m,n) = f(m,n) - f(m,n) * g(x,y;\eta_0)$, where $*$ indicates convolution. This high frequency component is then sent to the multi-channel filter bank for further decomposition in the frequency domain. The structure of the multi-channel filter bank is illustrated in Fig. 3, where h and h_0 represent the band-pass and low-pass filters, respectively. The output of the kth channel is denoted by $b_k(m,n)$, $0 \leq k \leq L$, and it can be considered as the band-limited contrast image. Both the center frequency and the bandwidth of the band-pass channel decrease as the channel index increases. Denote $B(k)$ be the L_2 norm of $b_k(m,n)$, that is given by

$$B(k) = \|b_k(m,n)\|_2 = \sqrt{\sum_{m=1}^{M}\sum_{n=1}^{M}[b_k(m,n)]^2} \quad (2)$$

We define the global band-pass image contrast of the kth channel, $C(k)$, by

$$C(k) = \frac{B(k)}{\sum_{i=1}^{L} B(i)} \quad (3)$$

where $0 \leq k \leq L$ and $\sum_{k=1}^{L} C(k) = 1$. Fig. 4 illustrates the behavior of the global band-pass image contrast for three different input images which were obtained from the UT Austin LIVE database [22]. Figs. 4 (a), (b), and (c) show the blurred versions of the Student Sculpture image, Lighthouse image, and Church and Capitol image using a circularly symmetric 2-D Gaussian function having a standard deviation of 0.53, 2.74, and 7.67, respectively. Fig. 4(d) shows the three curves of the global band-pass image contrast distributions for Figs. 4(a)-(c), where the red, blue, and green curves correspond to Fig. 4(a), Fig. 4(b), and Fig. 4(c), respectively. The three curves are monotonically decreasing with respect to the channel index. We are unable to differentiate different blurriness by examining these curves. We shall address this issue below.

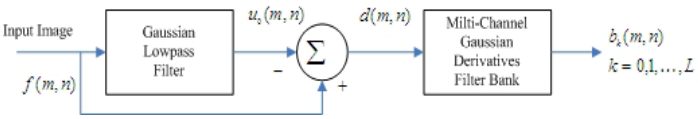

Figure 2. Extraction of high-pass component.

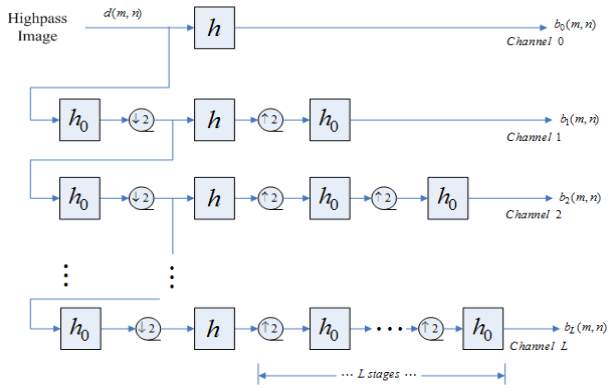

Figure 3. The structure of the multi-channel filter bank.

C. Channel Weighting

According to the idea of the matched filtering, the most significant channel is determined by channel comparison and then it is applied to compute the sharpness metric. We define the weighted global band-pass image contrast as

$$CW(k) = \frac{C(k)}{\|h_k(m)\|_2}, \quad k = 0,1,\cdots,L \tag{4}$$

where $h_k(m)$ is the equivalent one-dimensional impulse response of the kth band-pass channel. The most significant band-pass channel is determined by

$$k_{\max} = \arg\max\{CW(k), \quad k = 0,1,\ldots,L\} \tag{5}$$

The sharpness metric is given by

$$metric_{sharp} = \begin{cases} C(0) & , \quad k_{\max} = 0 \text{ or } 1 \\ C(1) & , \quad k_{\max} = 2 \\ C(2) & , \quad k_{\max} \geq 3 \end{cases} \tag{6}$$

The value of $metric_{sharp}$ is between 0 and 1. The sharper the image, the higher the metric is. Equivalently, the blurriness metric is defined by $metric_{blur} = 1 - metric_{sharp}$ Fig. 5 shows the three curves that represent the distributions of the weighted global band-pass image contrast of Figs. 4 (a)-(c). The red curve corresponding to Fig. 4(a) has a peak at $k_{\max}$ = 1. According to (6), the sharpness metric is 0.6995. The blue curve corresponding to Fig. 4(b) reaches maximum at $k_{\max}$ = 2, and the sharpness metric of this image is 0.327. Finally the green curve corresponding to Fig. 4(c) attains the maximum at $k_{\max}$ = 3, and the sharpness of this image is 0.16.

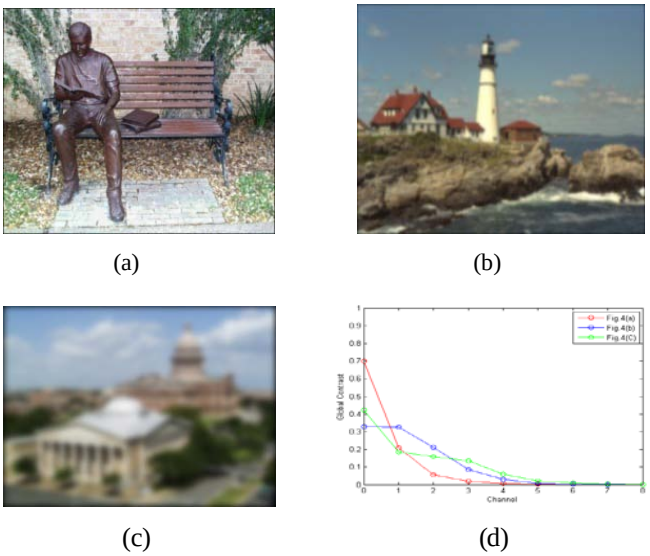

(a) (b)

(c) (d)

Figure 4. Three blurred images and their global band-pass image contrast distributions.

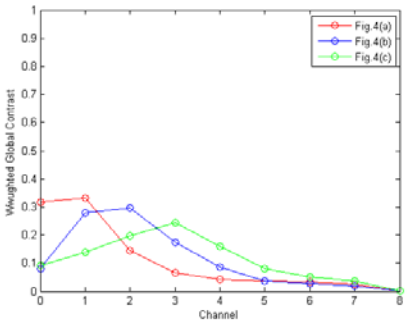

Figure 5. Three curves represent the distributions of weighted global band-pass image contrast of Figs. 4 (a)-(c).

IV. SIMULATION RESULTS

In this section, we present simulation results to illustrate the performance of the proposed no-reference sharpness metric. The performance of the proposed metric was tested with various Gaussian-blurred images from the LIVE database [22]. In order to validate the proposed objective no-reference sharpness metric, the simulation results are correlated with the subjective scores. We also compare the proposed metric to other popular no-reference sharpness metrics. The LIVE database consists of 29 color reference images (typically 768 × 512). A total of 145 Gaussian blurred images are generated from the reference images using a circular 2-D Gaussian kernel of standard deviation ranging from 0 to 15. The DMOS (differential mean opinion scores) subjective ratings of the blurred image quality are also available. DMOS values range between 0 and 100. The smaller the value, the higher the image quality is. To evaluate how well the metric values correlate with the provided DMOS values, we followed the suggestions of the VQEG report [23] where several evaluation criteria are proposed. A logistic fitting function is used, according to [23], to provide a nonlinear mapping between the objective and subjective scores to facilitate the subsequent correlation analysis. The adopted logistic fitting function is given by $DMOS_{pi} = \frac{\beta_1 - \beta_2}{1 + e^{(\frac{metric_i - \beta_3}{|\beta_4|})}} + \beta_2$, where β_1, β_2, β_3, and β_4 are the model parameters, $DMOS_{pi}$ is the predicted DMOS, and $metric_i$ is the objective metric for image i. Fig. 6 shows a scatter plot between the 145 proposed metrics ($metric_{blur} = 1 - metric_{sharp}$) and the corresponding 145 subjective ratings. The fitted curve is shown in red in Fig. 6. It is worthy to note that the fitted curve is close to a line. Thus, the proposed metrics are almost linearly related with the DMOS values. In fact, the nonlinear mapping could be discarded.

Given DMOS and $DMOS_{pi}$ values, the Pearson and Spearman correlation coefficients along with root mean-squared error (RMSE) were calculated as proposed by [23] to find out how well the proposed metric values match with the subjective test scores. The Pearson coefficient and RMSE indicate the prediction accuracy whereas the Spearman coefficient indicates the degree of monotonicity between the objective and the subjective scores. TABLE II summarizes the

correlation coefficients and RMSE for the proposed sharpness metric along with the metrics proposed in [2], [14], and [17]. It is clear from the results that the proposed metric correlates best with the subjective scores for the tested images as compared to other metrics. The resulting Pearson correlation coefficient of 0.931 from the proposed no-reference sharpness metric is quite noteworthy. As a comparison, full-reference quality-assessment methods (which require an original reference image) attain correlation coefficients of 0.784 (PSNR), 0.945 (SSIM), and 0.934 (VSNR) on these images [17].

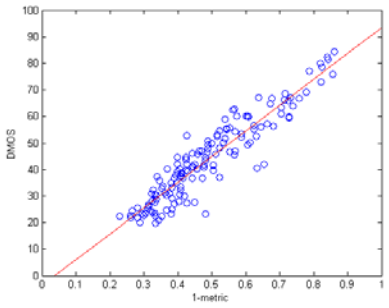

Figure 6. The scatter plot between the proposed metrics and the correpsonding DMOS subjective ratings. The red curve is fitted with $\beta_1 = 302.8749$, $\beta_2 = -728.4736$, $\beta_3 = -1.6674$, and $\beta_4 = -1.9717$.

TABLE II. PERFORMANCE COMPARISON OF THE SHARPNESS METRICS

	RMSE	Pearson	Spearman
Proposed $metric_{sharp}$	5.7218	0.9314	0.9224
JNB metric [2]	10.677	0.816	0.7871
CPBD metric [14]	6.9972	0.8955	0.9194
S_3 **metric [17]**	7.585	0.9143	unavailable

V. CONCLUSION

A no-reference image sharpness metric based on a filer bank of Gaussian derivative wavelets is proposed. Simulation results show the superiority of the proposed metric in terms of accuracy and monotonicity as compared to the existing metrics. The proposed metric is simple and fast. Future directions of research include investigating various types of blur such as anisotropic blur, circular blur, and space-variant blur.

REFERENCES

[1] Z. Wang and A. C. Bovik, Modern Image Quality Assessment, Synthesis Lectures on Image, Video & Multimedia Processing, Morgan & Claypool Publishers, 2006.

[2] R. Ferzli and L. J. Karam, "A no-reference objective image sharpness metric based on the notion of just noticeable blur (JNB)," IEEE Transactions on Image Processing, vol. 18, no. 4, pp. 717-728 , April 2009.

[3] X. Marichal, W.-Y. Ma, and H. Zhang, "Blur determination in the compressed domain using DCT information," in Proc. IEEE ICIP, vol. 2, pp. 386-390, 1999.

[4] C.-Y. Wee and R. Paramesran, "Measure of image sharpness using eigenvalues," Information Sciences, vol. 177, pp. 2533-2552, 2007.

[5] A. Maalouf and M.-C. Larabi, "A no reference objective color image sharpness metric," 18th European Signal Processing Conference (EUSIPCO-2010), Aalborg, Denmark, pp. 1019-1022, August 23-27, 2010.

[6] X. Zhu and P. Milanfar, "A no-reference sharpness metric sensitive to blur and noise," in 1st International Workshop on Quality of Multimedia Experience (QoMEX), San Diego, CA, vol. 2, no. 3, pp. 64–69, July 2009.

[7] Z. Wang and E. P. Simoncelli, "Local phase coherence and the perception of blur," in Adv. Neural Information Processing Systems (NIPS03), pp. 786–792, 2004.

[8] A. Ciancio, A. N. Targino, E. A. B. da Silva, A. Said, P. Obrador, and R. Samadani, "Objective no-reference image quality metric based on local phase coherence," IET Electronic Letters, vol. 45, no. 23, pp. 1162–1163, Nov. 2009.

[9] R. Hassen, Z. Wang, and M. Salama, "No-reference image sharpness assessment based on local phase coherence measurement," in Proc. IEEE ICASSP, pp. 2434-2437, March 14-19, 2010.

[10] H. Tong, M. Li, H. Zhang, and C. Zhang, "Blur detection for digital images using wavelet transform," in Proc. IEEE Int. Conf. Multimedia and Expo, vol. 1, pp. 17–20, Jun. 2004.

[11] P. Marziliano, F. Dufaux, S. Winkler, and T. Ebrahimi, "Perceptual blur and ringing metrics: applications to JPEG2000," Signal Processing: Image Communication , vol. 19, no. 2, pp. 163–172, Feb. 2004.

[12] E. P. Ong, W. S. Lin, Z. K. Lu, S. S. Yao, X. K. Yang, and L. F. Jiang, "No-reference quality metric for measuring image blur," in Proc. IEEE ICIP, vol. 1, pp. 469–472, July1-4, 2003.

[13] N. G. Sadaka, L. J. Karam, R. Ferzli, and G. P. Abousleman, "A no-reference perceptual image sharpness metric based on saliency-weighted foveal pooling," in Proc. IEEE ICIP, pp. 369-372 , Oct 12-15 , 2008.

[14] N. D. Narvekar and L. J. Karam, "A no-reference blur metric based on the cumulative probability detection (CPBD)," IEEE Transactions on Image Processing, vol. 20, no. 9 , pp. 2678-2683 , Sept. 2011.

[15] L. Liang, J. Chen, S. Ma, D. Zhao, and W. Gao, "A no-reference perceptual blur metric using histogram of gradient profile sharpness," in Proc. IEEE ICIP, pp. 4369-4372, Nov 7-10, 2009.

[16] J. Caviedes and F. Oberti, "A new sharpness metric based on local kurtosis, edge and energy information," Signal Processing: Image Communication, vol.18, no. 1, pp. 147-161, 2004.

[17] C. Vu and D. M. Chandler, "S_3: a spectral and spatial sharpness measure," MMEDIA, First International Conference on Advances in Multimedia, pp. 37-43, July 20-25, 2009.

[18] A. Ciancio, A. L. N. Targino da Costa, E. A. B. da Silva, A. Said, R. Samadani and P. Obrador, "No-reference blur assessment of digital pictures based on multi-feature classifiers," IEEE Transactions on Image Processing , vol. 20, no. 1, pp. 64-74, Jan. 2011.

[19] M.-J. Chen and A. C. Bovik, "No-reference image blur assessment using multiscale gradient," EURASIP Journal on Image and Video Processing, 2011:3, http://jivp.eurasipjournals.com/content/2011/1/3

[20] H. Liu and I. Heynderickx, "Issues in the design of a no-reference metric for perceived blur," IS&T/SPIE Electronic Imaging 2011 and Image Quality and System Performance VIII, 2011.

[21] C. Hsin, Y.-C. Chen, and S.-J. Shin, "Image reconstruction from edges based on a wavelet frame of gaussian derivatives," Visual Communications and Image Processing, pp. 1579-1589, 2005.

[22] H. R. Sheikh, A. C. Bovik, L. Cormack, and Z. Wang, LIVE Image Quality Assessment Database 2003 [Online]. Available: http://live.ece.utexas.edu/research/quality

[23] VQEG, Final Report From the Video Quality Experts Group on the Validation of Objective Models of Video Quality Assessment, Mar. 2000 [online]. Available: http://www.vqeg.org/